

## Repeatability study of helicopter-borne electromagnetic data

Haoping Huang<sup>1</sup> and Allen Cogbill<sup>2</sup>

### ABSTRACT

Helicopter-borne electromagnetic (EM) responses depend very much upon the altitude and plan-view flight path, especially when the resistivity of the terrain's materials varies laterally and/or vertically. Spatially consistent flight paths are required for repeatability analysis of the EM data. Caution should be used in examining the repeatability of the EM data because poor repeatability could result from spatially inconsistent flight paths. However, the apparent resistivity converted from the EM responses is virtually independent of the sensor altitude and directly reflects variations in the resistivity. Therefore, more meaningful repeatability analyses are achieved if the apparent resistivity is used instead of the EM response itself. We have analyzed 32 flights over a control line by using the EM amplitude, the phase, and the apparent resistivity. Our results show that the crosscorrelation for all 496 paired combinations of flights is better for the apparent resistivity than for the EM amplitude or phase. The apparent-resistivity data have average correlation coefficients from 0.89 to 0.94 as the frequency increases, whereas the amplitude and the phase data have average correlation coefficients from 0.78 to 0.85 without obvious frequency dependency.

### INTRODUCTION

An airborne electromagnetic (AEM) and magnetic survey was performed at Yucca Mountain, Nevada. A digital, helicopter-borne electromagnetic (HEM) system, GEM-2A, was employed along with a cesium-vapor magnetometer (Won et al., 2003). The HEM sensor uses a single transmitter coil and two receiver coils in a bucked configuration for multiple frequencies. The transmitter-receiver coil separation is 5.1 m. The survey used five frequencies: 450, 1290, 3690, 10,470, and 30,030 Hz. The purpose of this survey was to map the resistivity and magnetic susceptibility of the near-surface geology, to permit one to distinguish between volcanic tuffs

(which have relatively high remanent magnetization) and basaltic rocks (which have higher susceptibility than the tuffs). To perform a quality-control assessment for the magnetic and HEM data, a 5-km-long control line was flown in a west-to-east direction once per flight. The control line passes a hill formed by a thin (~25-m-thick) basalt lava flow underlain by alluvium. There were a total of 33 flights along the control line. In-flight navigation control employed a differential Global Positioning System (DGPS) with sub-meter horizontal accuracy 95% of the time using real-time DGPS transmissions. An onboard navigation system calculated the plan-view flight path to provide real-time flight-path guidance to the pilot. Bird altitude was measured by using a TRA 3000 radar altimeter with an accuracy of  $\pm 5\%$  at altitudes of 30–150 m.

AEM contractors usually re-fly some survey lines during production to check repeatability of electromagnetic (EM) data. Usually, a geophysicist visually checks the EM data from repeat flights to assess repeatability. If features on the EM data or the apparent resistivity show reasonable similarity, repeatability of the EM data is judged to be fine. Unfortunately, published studies on repeatability of AEM data are rare. Green and Lane (2003) presented the results of analyzing AEM data in which the same flight line had been flown repeatedly to monitor system performance. They described an approximate altitude correction method that assumes that there is a constant vertical response gradient for a given EM quantity for a short segment of the repeat line. A good measurement of the repeatability of AEM data was obtained after the altitude correction was applied. AEM data correction for altitude was tried in the early days of geophysical exploration (Dyck et al., 1974), but such correction has not been used by mainstream AEM contractors for a long time because AEM responses depend strongly upon the models and altitude ranges.

HEM responses depend very strongly upon the sensor altitude and plan-view flight path, especially when the resistivity structure varies laterally or vertically. Several major factors cause poor repeatability of AEM data: (1) inconsistent sensor altitude and plan-view flight path when the terrain resistivity is highly variable, (2) variations in sensor attitude, such as yaw, tilt, and roll in flight (Holladay et al., 1997; Fitterman and Yin, 2004; Yin and Fraser, 2004), (3) changes in calibration and/or unstable zero level over time (Fitterman, 1998;

Manuscript received by the Editor July 5, 2005; revised manuscript received May 4, 2006; published online October 5, 2006.

<sup>1</sup>Formerly Geophex, Ltd.; presently Geo-EM, LLC, 2001 Waterbrook Court, Raleigh, North Carolina 27603-5180. E-mail: haoping\_huang@hotmail.com.

<sup>2</sup>Los Alamos National Laboratory, MS F659 EES-3, Geophysics Group, Los Alamos, New Mexico 87545. E-mail: ahc@lanl.gov.

© 2006 Society of Exploration Geophysicists. All rights reserved.

Huang and Fraser, 1999), and (4) measurement errors that always appear in geophysical data. If calibration and zero level are well established and if the sensor works well, repeatability of HEM data will be affected mainly by variations in the sensor's altitudes and flight paths and measurement errors; the sensor-attitude errors are second-order effects. In fact, a repeatability check of HEM data should be based on not only the EM responses but also the apparent resistivity computed from EM responses by using the pseudolayer model (Fraser, 1978). Such an approach minimizes the effects caused by variations in the altitudes and flight paths as long as the resistivity of the terrain along a repeat line does not change dramatically laterally or vertically.

In this paper, we report the repeatability of HEM data from 32 flights over the control line; the repeatability was determined by using crosscorrelation of the EM amplitude, the phase, and the apparent resistivity. The purpose of this study is to ascertain the consistency of the digital broadband HEM data, which is part of quality-control assessment. This study is limited to data repeatability and does not include other aspects of quality-control assessments, such as systematic error and accuracy. We hope that results from this study may help HEM users evaluate their data for further interpretations.

### THE CLOSENESS OF FLIGHT PATHS

HEM data reflect only the near-surface geology, the lateral coverage is limited, and the magnitude of EM response decreases dramatically with increasing distance between sensor and source. Therefore, small variations in the sensor altitude or plan-view flight path may cause considerable change in EM response, even if resistivity of the terrain's materials does not change. Repeatability analysis of the EM response is meaningful only when the altitudes and flight paths are close to each other.

We examine the closeness of the altitudes and plan-view flight paths on which repeatability analysis of EM responses is based. The EM data are affected differently by horizontal and vertical variations in the flight path. The horizontal closeness of the plan-view flight paths can be broken into two parts: inline (in the direction of the flight line),  $d_x$ , and transverse (perpendicular to the flight line),  $d_y$ .

The inline variation is ignored because of interpolation of the data along the flight line. Thus, we only consider the transverse component of variation  $d_y$  in plan-view flight paths, which is

$$d_y = \frac{1}{N} \sum_{k=1}^N |y_{ik} - y_{jk}|. \quad (1)$$

Similarly, the vertical closeness of two flight paths is

$$d_z = \frac{1}{N} \sum_{k=1}^N |z_{ik} - z_{jk}|. \quad (2)$$

In equations 1 and 2,  $N$  is the number of data points in the control line, the  $y_{ik}$  values are taken from the DGPS data, and the  $z_{ik}$  values are the radar altimeter readings. The subscripts  $i$  and  $j$  stand for the flights, and  $k$  indicates the data station. The total closeness of the flight paths of two flights can be written as average distance  $d$ ,

$$d = \frac{1}{N} \sum_{k=1}^N \sqrt{(y_{ik} - y_{jk})^2 + (z_{ik} - z_{jk})^2}. \quad (3)$$

Figure 1a illustrates plan-view flight paths for all 33 flights along the control line. One flight deviated significantly from the others at the beginning of the line; therefore, in the following analysis, this flight is ignored. The bold black line in the middle represents the average plan-view flight path; its maximum deviation is about  $\pm 20$  m. The standard deviation is 6–10 m (Figure 1b); the maximum value occurs at the beginning of the line.

Figure 1c presents the sensor altitudes, and Figure 1d shows their standard deviations. The altimeter readings, generally about 40 m, are smaller over the hill formed by the lava flow and larger away from the hill. The standard deviations range from 3.5 to 6.5 m.

The minimum mean distance between two flights is 5.2 m, and the maximum is 20.6 m (equation 3).

### METHOD

As already indicated, helicopter-borne EM responses are dependent on the sensor altitude and plan-view flight path. Our analysis of these two parameters could be qualitative or semiquantitative.

One way of comparing two data series is to fit one to the other. The goodness of fit, measured in some manner, would be an index to their similarity. Such an approach is in effect done by the process of crosscorrelation. The correlation coefficient  $r$  is a measure of the degree of correlation of two data sequences:

$$r = \frac{\text{COV}_{ij}}{s_i s_j}, \quad (4)$$

where  $\text{cov}_{ij}$  represents the covariance of the two data sequences and  $s_i$  and  $s_j$  are the standard deviations of the sequences  $i$  and  $j$ . Also, a linear regression equation can be established between the two data sets. The slope  $a$  and  $y$ -intercept  $b$  of the linear equation can be determined from the data. If two sequences of data match perfectly, the cor-

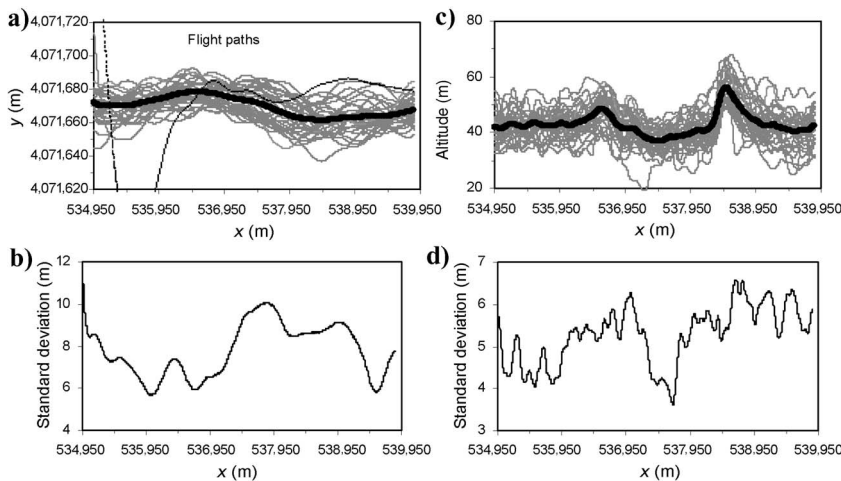


Figure 1. (a) Plan-view flight paths. (b) Standard deviations of plan-view flight paths. (c) Sensor altitudes. (d) Standard deviations of sensor altitudes. The lines in bold black in (a) and (c) stand for the average flight path and altitude, respectively. The control line begins at  $x = 534,950$  and ends at  $x = 539,950$ .

relation coefficient  $r$  equals 1, slope  $a$  equals 1 and  $y$ -intercept  $b$  equals 0.

Measurements obtained by helicopter-borne EM systems are the in-phase ( $I$ ) and quadrature ( $Q$ ) components of the secondary magnetic field. However, repeatability analysis may not be carried out by using the  $I$  and  $Q$  because the phase angle  $\alpha = \arctan(Q/I)$  would be ignored, which is the most important variable in terms of interpretation of the EM data. Therefore, the amplitude  $A = (I^2 + Q^2)^{1/2}$  and phase angle  $\alpha$  are both used in this study. Both  $A$  and  $\alpha$  depend upon the sensor altitude. The third parameter we use in our analysis is the apparent resistivity, which is computed from  $I$  and  $Q$  or from  $A$  and  $\alpha$  through the pseudolayer half-space model developed by Fraser (1978). This algorithm yields the apparent resistivity and the apparent sensor-source distance or apparent height. The measured sensor altitude is not used, as it commonly contains errors such as those caused by a forest canopy. Therefore, errors in altimeter readings do not corrupt the computed resistivity for the pseudolayer model. The apparent height is merely an artifact to account for differences from measured bird altitude. Magnetic susceptibility in this area affects the in-phase component at the lowest frequency, which is computed from the in-phase response at the resistive limit and included in the apparent resistivity computation (Huang and Fraser, 1998, 2000).

For each flight, EM data were obtained over the control line. Then the bird was flown to a height well above the ground surface (200–300 m) to collect data for a zero-level correction. A standard preliminary processing was applied to the data, including low-pass filtering to remove random noise and constant zero-level shifts, i.e., EM responses obtained at high altitude were subtracted from those obtained at the lower level of the control-line surveys. Drift was ignored because there were only about 2 minutes of flying over the control line. Then, EM data were transformed to the apparent resistivity. Finally, crosscorrelation of the EM amplitude, the phase, and the apparent resistivity was performed for all 496 paired combinations from 32 flights.

### RESULTS

We show the results from two pairs of flights in detail. One pair of flights (F3 and F8) has the minimum mean distance between their flight paths, and the other (F5 and F14) has the maximum mean distance. Then, we show briefly the results of the crosscorrelation for all 496 paired combinations from 32 flights.

Flights F3 and F8 have the least average separation. Figure 2 shows plan-view flight paths, altitudes, and distances between F3 and F8. The mean distance (from equation 3) is 5.2 m. Figure 3 presents profiles of the amplitudes, the phase angles, and the apparent resistivities for the two flights. Altitude determined by radar altimeter is shown again to help examine the amplitude because amplitude variations are often caused by changes in altitude instead of geology. For example, the high-amplitude response observed in the middle of the line is caused by the small terrain clearance of the sensor while flying over the top of the hill. Amplitude and phase for the two flights

are similar even though the amplitudes are not comparable owing to the different terrain clearance during the two flights. The apparent resistivity profiles calculated from the EM data are comparable and have similar features. Over the alluvium, the apparent resistivity var-

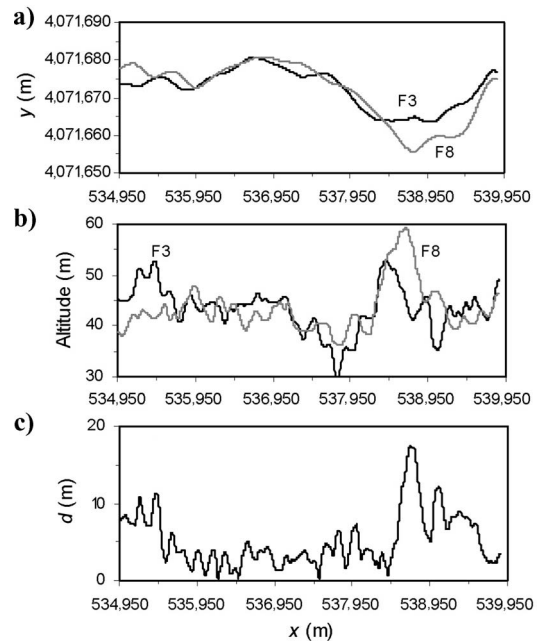


Figure 2. (a) Plan-view flight paths. (b) Sensor altitudes. (c) Distances between flight paths F3 and F8.

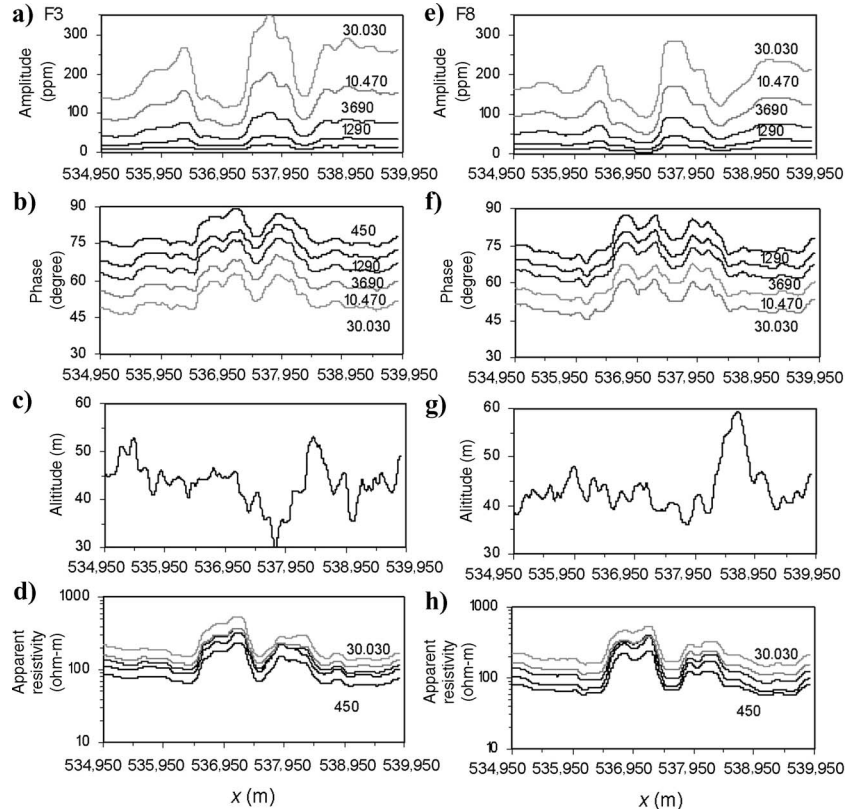


Figure 3. Profiles of amplitudes, phases, bird altitudes, and apparent resistivities from (a–d) flight F3 and (e–h) flight F8. Labels on curves indicate frequencies.

ies from about 100 to 200 ohm-m. It is >200 ohm-m over the basalt. The fact that the apparent resistivity increases with the frequency indicates that the terrain's materials are more conductive at depth than near the surface.

Figure 4 shows scatter diagrams of the EM amplitudes, the phases, and the apparent resistivities for flight F3 plotted versus flight F8 at five frequencies. The slope  $a$  and  $y$ -intercept  $b$  of the linear equation are also labeled in each scatter diagram along with the correlation coefficient  $r$ . If the parameters from the two flights matched perfectly, all data would be on the straight diagonal line from the lower-

left corner to the upper-right corner and would yield correlation coefficient  $r = 1$ , slope  $a = 1$ , and  $y$ -intercept  $b = 0$ . The fact that, for these two flights, the correlation coefficients for  $A$  and  $\alpha$  are >0.85 at all frequencies indicates that the response from one flight correlates well with the other. Correlation coefficients for apparent resistivity itself vary from 0.98 to 0.94 as the frequency decreases; all slopes are close to 1, and the  $y$ -intercepts are relatively small. It is obvious that the correlation between the two flights is better for the apparent resistivity than for the EM response itself.

The flight paths of flights F5 and F14 are separated by the maximum distance. The mean distance between the two flight paths is 20.6 m, as shown in Figure 5. Figure 6 presents profiles of the amplitudes, phases, altimeter readings, and apparent resistivities. The apparent resistivities measured during the two flights demonstrate the same features, even though the EM data looked disparate because of the distance between the two flight paths. Figure 7 shows scatter diagrams of the EM amplitudes, the phases, and the apparent resistivities for flight F5 plotted against flight F14 at five frequencies. The correlation coefficients for the amplitude and phase range from 0.64 to 0.73, which is much lower than those for flights F3 and F8. However, compared to these data, the correlation of the apparent resistivity converted from the EM data is much better, as shown in Figure 7c. The correlation coefficients range from 0.89 to 0.93. As has been shown in Figures 3 and 6, features of the EM amplitude commonly reflect variation in sensor altitude rather than in the geology, whereas the apparent resistivity is directly related to the geology.

Results of the crosscorrelation for all 496 paired combinations from 32 flights are shown in Figure 8 as plots of the average correlation coefficients over all frequencies for the amplitudes, the phases, and the apparent resistivities. The  $x$ - and  $y$ -axis labels are the flight numbers, and the correlation coefficient for any two flights is presented as a colored dot. The magenta dots stand for high correlation coefficients, and the blue spots stand for low correlation coefficients, as indicated by the color bar. From these plots, we can determine which flight yielded significantly different results from the others. For example, the amplitude of flight 11 differs from the others, as shown by the fact that the correlation coefficients between flight 11 and the others are low, which is indicated by the blue dots. Flight 4 is poorly correlated with the others in terms of the phase. The apparent resistivity has higher correlation coefficients, but the apparent resistivity measured during flight 28 is not as good as the others.

We have listed the mean values of the correlation coefficients  $r$ , slopes  $a$ , and  $y$ -intercepts  $b$  for the amplitude and phase data (Table 1) and for the apparent resistivity data (Table 2) at the five frequencies studied. The correlation coefficients range from 0.78 to 0.85 for amplitude and phase and from 0.89 to 0.94 for the apparent resistivity. Because the mean slope is close to one and the  $y$ -intercept is small for the apparent resistivity, the values of apparent resistivity agree well with each other.

Correlation coefficients for each pair of flights (496 total pairs) are associated with a horizontal distance  $d_y$  and vertical distance  $d_z$  (equations 1 and 2). Thus, we can plot the correlation coefficients

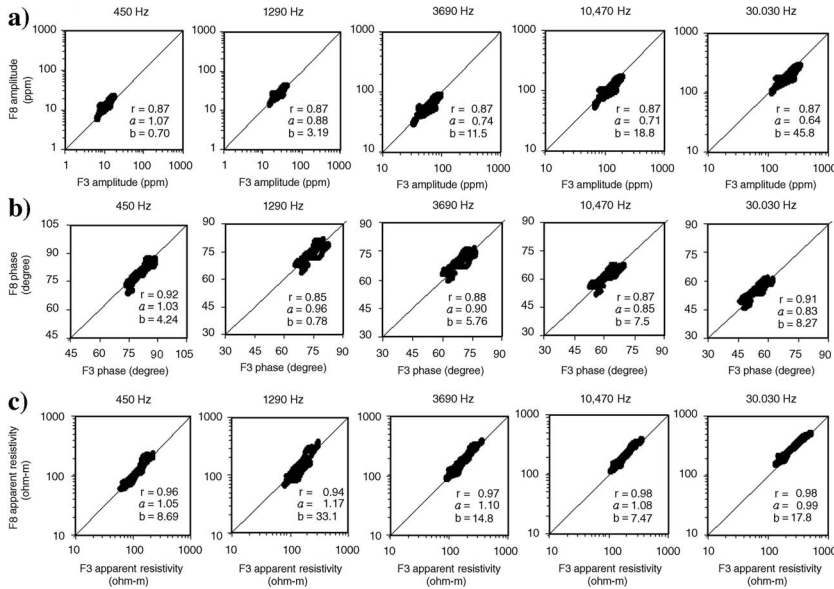


Figure 4. Scatter diagrams of amplitudes, phases, and apparent resistivities at five frequencies for flight F3 versus flight F8. Shown on each plot are the correlation coefficients  $r$  and best-fit parameters  $a$  and  $b$ . Diagonals are 1:1 correlation lines ( $y = x$ ).

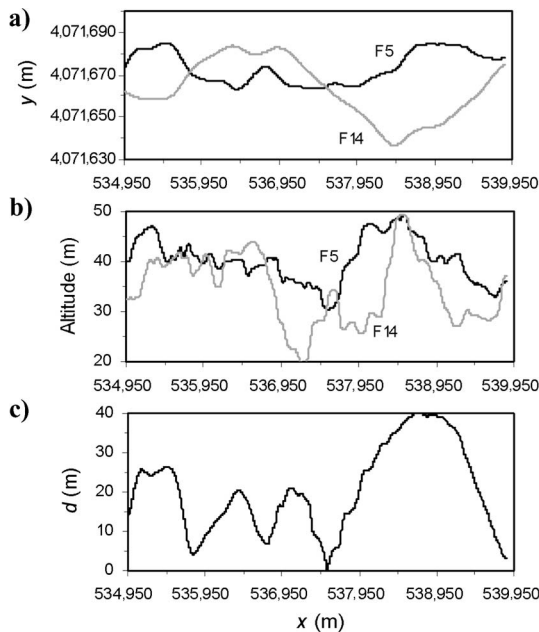


Figure 5. (a) Plan-view flight paths. (b) Sensor altitudes. (c) Distances between flight paths of flight F5 and flight F14.

against  $d_y$  and  $d_z$ . An obvious tendency for a specific parameter plotted against  $d_y$  or  $d_z$  indicates that the parameter depends strongly upon  $d_y$  or  $d_z$ . Figure 9 illustrates correlation coefficients at five frequencies for all 496 paired combinations plotted against the horizontal distance  $d_y$  and vertical distance  $d_z$ . The gray lines stand for the

trend line that linearly fits the data and statistically reflect the relationships between horizontal or vertical distances and correlation coefficients. The slope of the trend lines has less dependence on horizontal distance than on vertical distance; this finding indicates that data repeatability is affected mainly by the vertical distance. The slope of the trend line against  $d_z$  decreases going from amplitude to phase to apparent resistivity, i.e., the apparent resistivity data are virtually independent of variations in sensor altitude.

As described, the apparent resistivity is statistically independent of the altitudes and flight paths. However, we have not obtained a perfect match of the apparent resistivity measurements during the repeated flights, and the correlation coefficients between certain pairs of flights are even lower than 0.8, as shown in Figure 9. The reasons for the poor repeatability could be (1) variations in the sensor's attitude, such as yaw, pitch, and roll in flight, (2) residual leveling and/or calibration errors, and (3) measurement errors that al-

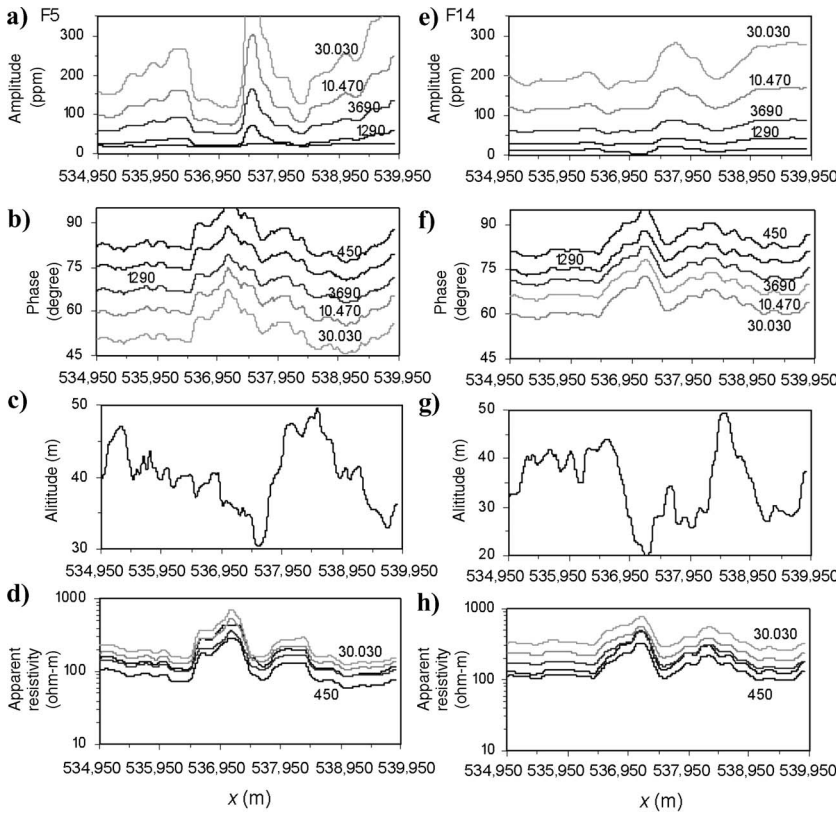


Figure 6. Profiles of amplitudes, phases, bird altitudes, and apparent resistivities from (a-d) flight F5 and (e-h) flight F14. Labels on curves indicate frequencies.

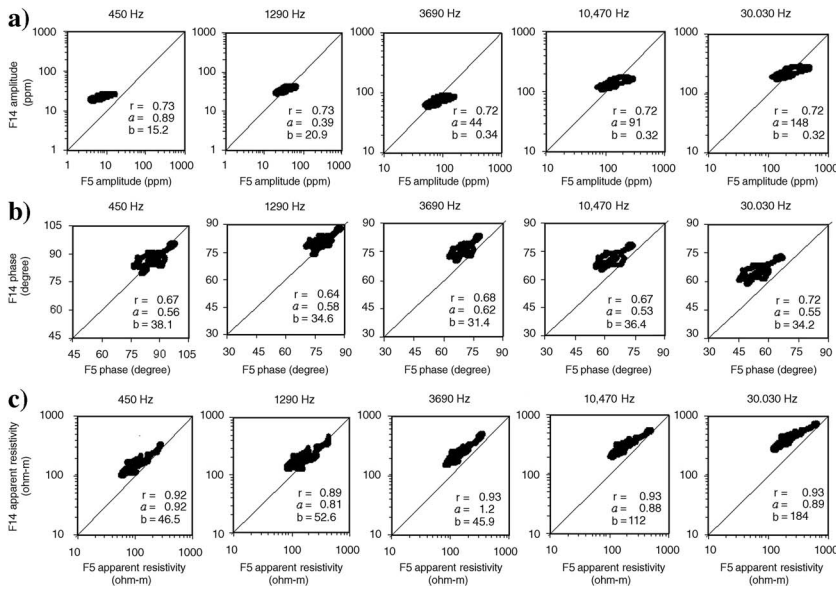


Figure 7. Scatter diagrams of amplitudes, phases, and apparent resistivities at five frequencies for flight F5 vs. flight F14. Shown on each plot are the correlation coefficients  $r$  and best-fit parameters  $a$  and  $b$ . Diagonals are 1:1 correlation lines ( $y = x$ ).

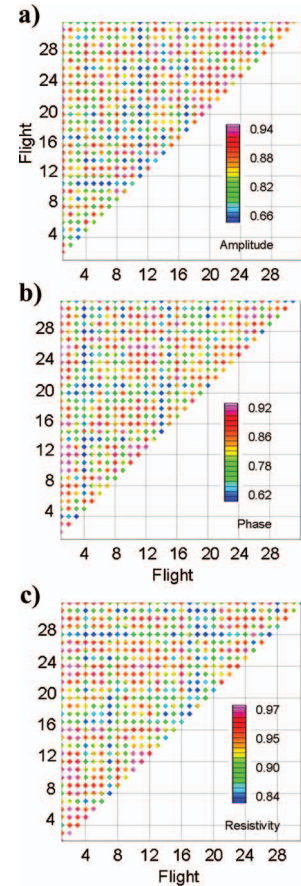


Figure 8. Correlation coefficients for (a) the amplitude, (b) the phase, and (c) the apparent resistivity for all frequencies. The numbers on the  $x$ - and  $y$ -axes are the flight numbers, and the correlation coefficient for any two flights is presented as a colored dot. The magenta dots stand for high correlation coefficients, and the blue spots stand for low correlation coefficients, as indicated by the color bar.

**Table 1. The mean values of the correlation coefficients  $r$ , slope  $a$ , and  $y$ -intercept  $b$  for the amplitude  $A$  and phase  $\alpha$  of the EM data at five frequencies.**

	450 Hz		1290 Hz		3690 Hz		10,470 Hz		30,030 Hz	
	$A$	$\alpha$	$A$	$\alpha$	$A$	$\alpha$	$A$	$\alpha$	$A$	$\alpha$
$r$	0.80	0.78	0.84	0.80	0.85	0.82	0.85	0.78	0.85	0.82
$a$	0.92	0.29	0.86	0.23	0.86	0.78	0.86	0.81	0.86	0.80
$b$	3.0	53.6	7.06	17.7	10.4	12.9	15.7	12	23.9	8.23

**Table 2. The mean values of the correlation coefficients  $r$ , slope  $a$ , and  $y$ -intercept  $b$  for the apparent resistivity at five frequencies.**

	450 Hz	1290 Hz	3690 Hz	10,470 Hz	30,030 Hz
$r$	0.89	0.90	0.93	0.93	0.94
$a$	0.84	1.13	1.09	1.04	1.02
$b$	-36.6	14.2	2.45	0.27	-2.67

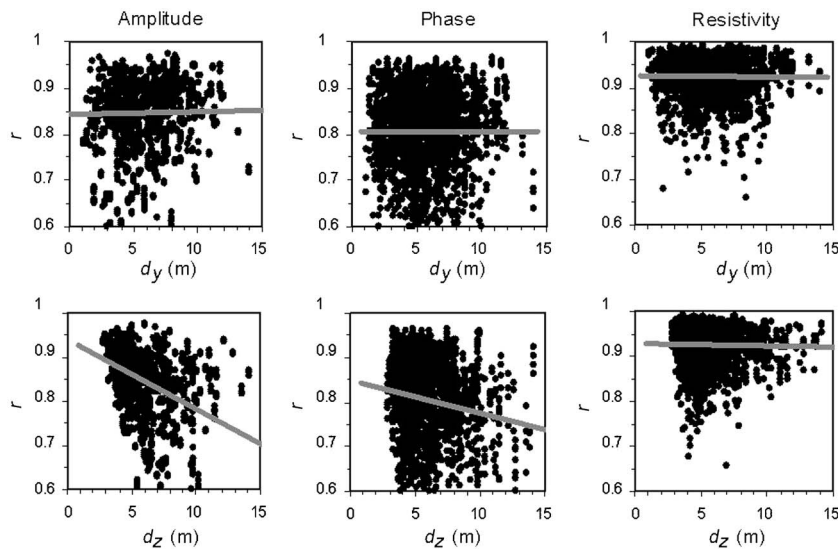


Figure 9. Correlation coefficients,  $r$ , at the five frequencies for all 496 paired combinations plotted against the average horizontal distance,  $d_y$ , and vertical distance,  $d_z$ , between flights. The gray lines are linear trend lines that fit the data.

ways appear in geophysical data. We have ignored possibilities 1 and 2 in this study. However, the quality of the EM data and apparent resistivity may be improved by considering these factors (Holladay et al., 1997; Deszcz-Pan et al., 1998; Fitterman and Yin, 2004; Yin and Fraser, 2004).

## CONCLUSIONS

HEM responses depend very much upon the sensor altitude and plan-view flight path, especially when the resistivity of the terrain's materials varies laterally and/or vertically. Therefore, spatially consistent flight paths are required for repeatability analysis of the EM

data. Caution should be used in examining repeatability of the EM data because poor repeatability could result from flight-path variations. The apparent resistivity converted from the EM responses is virtually independent of sensor altitude and directly reflects variations in resistivity of the terrain's materials. Therefore, repeatability analysis is more meaningful if the apparent resistivity is used instead of the EM response itself.

We have analyzed 32 repeating flights over a control line through the use of (1) the EM amplitude, (2) the phase, and (3) the apparent resistivity. Our results show that crosscorrelation for all 496 paired combinations of flights is better for the apparent resistivity than for the EM amplitude or phase. The average correlation coefficients over 496 flight-path pairs vary from 0.89 to 0.94 for the apparent resistivity as the frequency increases and from 0.78 to 0.85 for the EM amplitude or phase without obvious frequency dependency.

## ACKNOWLEDGMENTS

We are grateful to I. J. Won for his valuable comments and suggestions. We also thank the associate editor and the anonymous reviewers for their important comments and suggestions.

## REFERENCES

- Deszcz-Pan, M., D. V. Fitterman, and V. F. Labson, 1998, Reduction of inversion errors in helicopter EM data using auxiliary information: *Exploration Geophysics*, **29**, 142–146.
- Dyck, A. V., A. Becker, and L. S. Collett, 1974, Surficial conductivity mapping with the airborne INPUT system: *Canadian Mining and Metallurgical Bulletin*, **67**, April, 1–6.
- Fitterman, D. V., 1998, Sources of calibration errors in helicopter EM data: *Exploration Geophysics*, **29**, 65–70.
- Fitterman, D. V., and C. Yin, 2004, Effect of bird maneuver on frequency-domain helicopter EM response: *Geophysics*, **69**, 1203–1215.
- Fraser, D. C., 1978, Resistivity mapping with an airborne multicoil electromagnetic system: *Geophysics*, **43**, 144–172.
- Green, A., and R. Lane, 2003, Estimating noise levels in AEM data: ASEG, 16th Geophysical Conference and Exhibition, Extended Abstract, Preview, 70.
- Holladay, J. S., B. Lo, and S. J. Prinsenber, 1997, Bird orientation effects in quantitative airborne electromagnetic interpretation of pack ice thickness sounding: *Oceans'97*, Marine Technology Society/IEEE Conference Proceedings, 2, 1114–1119.
- Huang, H., and D. C. Fraser, 1998, Magnetic permeability and electrical conductivity mapping with a multifrequency airborne EM system: *Exploration Geophysics*, **29**, 249–253.
- , 1999, Airborne resistivity data leveling: *Geophysics*, **64**, 378–385.
- , 2000, Airborne resistivity and susceptibility mapping in magnetically polarizable areas: *Geophysics*, **65**, 502–511.
- Won, I. J., A. Oren, and F. Funak, 2003, GEM-2A: A programmable broadband helicopter-towed electromagnetic sensor: *Geophysics*, **68**, 1888–1895.
- Yin, C., and D. C. Fraser, 2004, Attitude corrections of helicopter EM data using a superposed dipole model: *Geophysics*, **69**, 431–439.